Physics-Informed Compact Model for SF_6/O_2 Plasma Etching

Lado Filipovic[1,2*], Josip Bobinac[2], Julius Piso[2], Tobias Reiter[1,2]
[1]CDL for Multi-Scale Process Modeling of Semiconductor Devices and Sensors at the
[2]Institute for Microelectronics, TU Wien, 1040 Vienna, Austria
*Email: filipovic@iue.tuwien.ac.at

***Abstract*—We propose a process simulation/emulation flow which incorporates the generation and application of compact models for fast geometry generation, suitable for design-technology co-optimization (DTCO). The methodology is applied to develop a compact model for etching in a SF_6/O_2 plasma using 35 data points from experimental measurements and results from a calibrated physical model. The compact model is tested against physical simulations using 80 random points in the input parameter domain consisting of varying the oxygen content and pressure in the plasma chamber. The model is shown to produce highly accurate geometries with an average error for the depth and width at half depth (WAHD) of 2.0% and 1.0%, respectively. The simulation speedup is more than three orders of magnitude, when compared to the physical model; it should also be noted that the parallelized physical model was executed on 40 cores, while the compact model was run on a single core.**

***Index Terms*—process simulation and emulation, design-technology co-optimization (DTCO), technology computer-aided design (TCAD), SF_6/O_2 etching, compact model**

I. Introduction

Technology computer aided design (TCAD) has become an essential tool to assist in the development and optimization of micro- and nanoelectronic devices. Specifically when it comes to the integration of novel materials and fabrication processes, the use of TCAD in the design-technology co-optimization (DTCO) cycle has become indispensable [1], [2]. To enhance the performance of semiconductor-based devices and circuits, designers need to understand how even a single step in the fabrication process affects the device geometry and ultimately the circuit operation, reliability, and variability. This understanding enables the circuit designer to give feedback to the fabrications engineer, who can modify the process to improve circuit performance. However, relying solely on experiments to establish this feedback loop involves extreme time and cost considerations. Hence, it is critical to integrate process simulations with device and circuit simulations through TCAD-supported DTCO to design future semiconductor devices and technologies successfully [3].

Nevertheless, a critical problem with a DTCO implementation from fabrication to circuit is that the generation of process-aware geometries using physical process models typically requires noisy stochastic models and is very time intensive [4]. The inclusion of equipment parameters in the simulation adds further complexity since equipment-level and wafer-level simulations require drastically different length scales [5]. Therefore, there is a need to provide geometries which capture the relevant equipment settings in a fast way for DTCO [6].

In our previous studies, we have implemented geometric advection [7] and analytical geometric representations [6] for fast process-aware structure generation. In this study, we expand on these concepts by introducing a workflow which links equipment parameters and measurements to relevant processes and we develop a compact model for plasma etching of a cylindrical hole in an SF_6/O_2 chemistry to show the capabilities of the implemented approach. Ultimately, this method allows for the quick generation of three-dimensional (3D) structures, which can be integrated within a larger logic cell or circuit design very quickly and efficiently, while considering the equipment parameters required to generate such a structure.

II. Simulation Flow

The flow used by the framework to generate and apply physical and compact models is provided in Fig. 1. Each arrow and number combination corresponds to a particular process in this sequence:

1) The collection of relevant data $\mathbf{x}$ from experimental observations. Here, we also determine which features are important in the final geometry so that these are reproduced with the compact model $\mathbf{f(x)}$.
2) The experimental parameters and features are used to calibrate the physical model. The physical model typically requires several parameters to

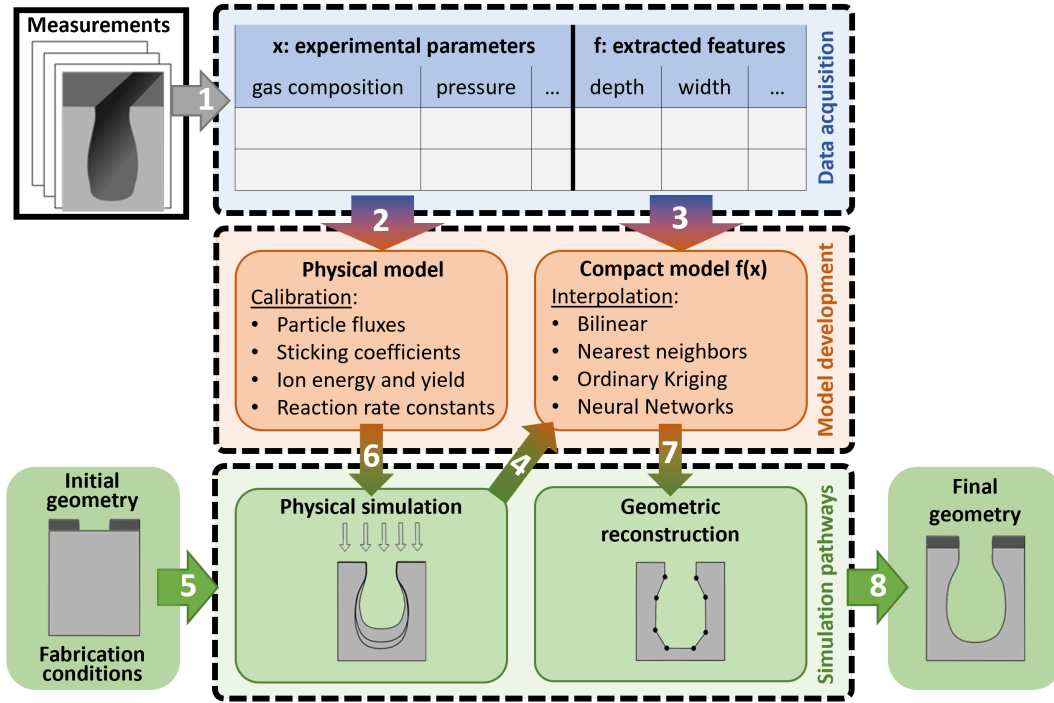

Fig. 1. Model generation, including the calibration of physical models (steps 1 and 2) and training of compact models (steps 1, 3, and 4). The simulation flows for both physical (steps 5, 6, and 8) and compact (steps 5, 7, and 8) modeling are likewise provided.

properly describe the particles in the chamber, the material being deposited or etched, and the interactions between the two in time.

3) The compact model is likewise devised or trained using the experimental data. However, the primary goal here is to find a relationship between the equipment parameters and the extracted features. This can be done using compact models where geometry features are represented with polynomials, or trained machine learning (ML) models, such as neural networks (NN) approaches.
4) Due to the often limited availability of experimental data, compact model training can be supported by physical simulations. This way, the compact model can also be used for extrapolation beyond the experimental data set.
5) A simulation run is initiated by providing the initial geometry and input parameters. The user must also identify whether a physical simulation or geometric reconstruction is desired.
6) If a physical simulation is chosen, a simulation is carried out using the calibrated physical model.
7) Alternatively, if a geometric reconstruction is chosen, a compact model is applied using an appropriate interpolation scheme.
8) Finally, the end geometry is provided as the output of the simulation initiated in step 5.

III. Compact Model

The experimental results from Belen et al. [8] and the SF_6/O_2 physical model described in [4] are combined to generate the compact model. The experimental parameters used in this study are the proportion of oxygen in the feed gas composition y_{O_2}, with respect to the SF_6/O_2 concentration, and the pressure in the plasma chamber P. For the generation of the compact model, we extract 35 data points from combined experimental results (bold font) and physical simulation (normal font), while varying the feed gas composition from $y_{O_2} = 0.44$ to $y_{O_2} = 0.63$: (**0.44**, **0.50**, 0.53, **0.56**, 0.58, 0.60, **0.63**) and the pressure from $P = 10\,\mathrm{mTorr}$ to $P = 40\,\mathrm{mTorr}$: (**10**, 17.5, **25**, 32.5, **40**). These data points represent the final simulated structures and span a rectilinear grid from which any point can be taken as input, shown in Fig. 2.

Geometric features are extracted from the sample structures to generate the final geometry for each of the defined (blue) points in Fig. 2. In this case, final depth and profile widths are measured at specific locations down the etched cylindrical hole, as shown in Fig. 3(a) for a sample measurement at $(y_{O_2}, P) = (0.44, 25\,\mathrm{mTorr})$. First, the profile is extracted, c.f. Fig. 3(b), or generated using physical simulations, then a point cloud of the geometry is created which represents the final geometry. Since, in this ex-

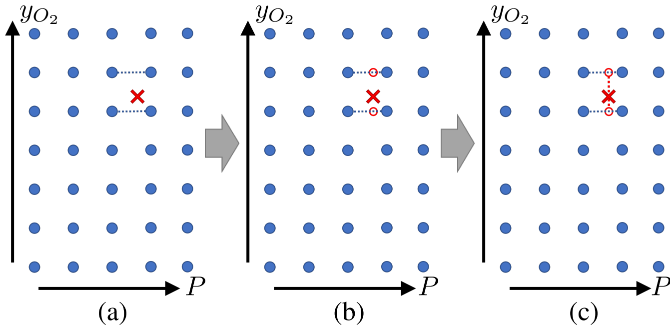

Fig. 2. Illustration of bilinear interpolation. After locating the corresponding rectangle in (a), an interpolation of the geometric features along each coordinate axis is performed, shown in (b). Another interpolation round in (c) is performed between the newly generated points to obtain the values at the target location.

ample, we are analyzing a cylindrical hole, we limit the compact model to represent the radius of the hole at a desired number of points along the vertical direction, as shown in Fig. 3(c). This simplifies the problem to a two-dimensional (2D) rotational structure instead of a full 3D representation.

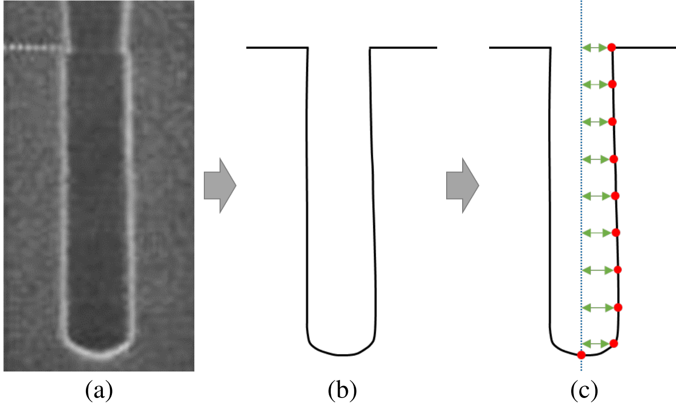

Fig. 3. Extracted geometric profile in a cylindrical trench from (a) experimental measurements (Reprinted with permission from [8]. Copyright 2005, American Vacuum Society). The profile is extracted in (b) which is then represented using a series of points along the vertical direction, representing the radius in (c). A cubic spline interpolation is chosen to represent the geometry between the points.

IV. Results and Discussion

When running the compact model (cf. Fig. 1: flow 5→7→8), the final geometry is constructed using bilinear interpolated geometric values of the radial widths at specific pre-defined depths. The generated points of the new arbitrary surface can be used to form a 3D hole profile by rotating the radii around the central rotation axis, as illustrated in Fig. 4. This way, the bowing effects, typically encountered in plasma etching, can be replicated with the compact model. The final points are then connected into a mesh to construct the final geometry, which can be combined within a large 3D process-aware structure for further processing or for parasitic parameter extraction [6]. Since the compact model requires no time stepping, the geometric reconstruction is much faster than performing a physical model, with a time of 0.5 s compared to 1163 s (average of 10 physical simulations), respectively (see Table I). The simulation were executed on a DELL PowerEdge R740 server with an Intel Xeon Gold 6248 processor. The physical simulation was executed parallelized on 40 cores while the compact model ran on a single core.

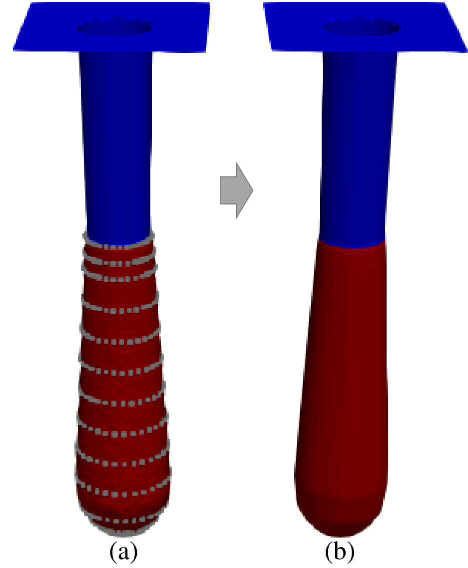

Fig. 4. Maximum depth and radii at specific depths are measured for the simulated samples. Radii and maximum depth are interpolated as described by Fig. 2. Further points which are used for the construction of the final geometry are obtained by rotational symmetry; (a) shows a strong agreement between the points obtained and the geometry from a physical simulation, and (b) shows the final constructed geometry by connecting the calculated points.

TABLE I
SIMULATION TIME (AVERAGE OF 10 SIMULATIONS) TO GENERATE AN ETCHED PROFILE IN A CYLINDRICAL HOLE.

Model	**Simulation time**	**Hardware use**
Physical:	1163 s	40 cores
Compact:	0.5 s	Single core

In order to assess the accuracy of the compact model, 80 randomly selected chamber parameter pairs are taken from the considered grid from Fig. 2. The relative error in the final depth and in the width at half depth (WAHD) of the generated cylindrical hole is determined using E_{rel}

$$E_{\text{rel,x}} = \frac{\text{x}_{\text{physical}} - \text{x}_{\text{compact}}}{\text{x}_{\text{physical}}} \cdot 100\%, \tag{1}$$

where x represents a geometrical property, such as the hole depth or the WAHD. The results of the eighty

random samples indicate whether the value was over- or underestimated and are provided in Fig. 5. The average relative error for the depth is $E_{\text{rel,depth}} = 2.0\%$ with a maximum relative error of 6.2%. For the WAHD, the numbers are quite similar, with the average relative error being $E_{\text{rel,WAHD}} = 1.0\%$ and the maximum being 6.2%. (see Table II). These relatively low error margins suggest that this purely geometric approach with a straightforward interpolation scheme can nevertheless produce reasonable geometries. With the presented method, we can replace time- and compute-intensive physical simulations in a DTCO flow. Recent estimates suggest that the integration of machine learning approaches in semiconductor fabrication can lead to a cost saving of up to 50% for finFET technologies [2]. To increase the number of analyzed input parameters, a different interpolation approach should be used, such as nearest neighbour interpolation, in order to reduce the number of initial experimental measurements which are required to have reasonable model accuracy.

TABLE II
CALCULATED ERROR IN THE GEOMETRY OF THE PROPOSED COMPACT MODEL AFTER 80 RANDOM INTERPOLATIONS.

Property	Average error	Maximum error
Depth	2.0%	6.2%
WAHD	1.0%	6.2%

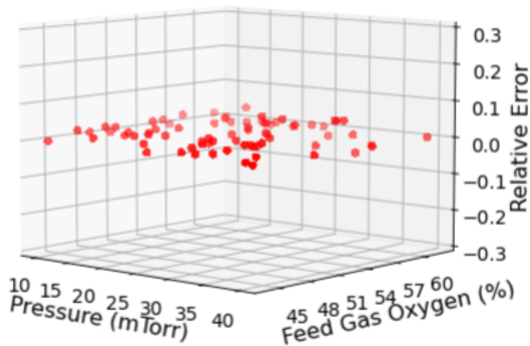

(a) Relative error for the etched hole depth

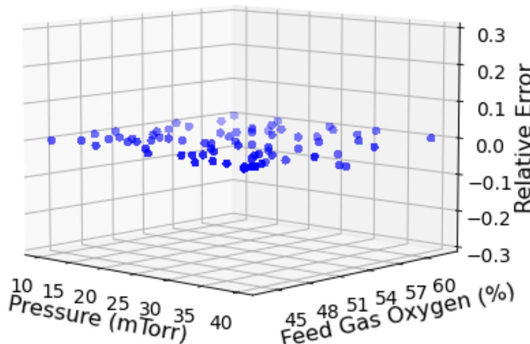

(b) Relative error for the WAHD

Fig. 5. 3D plots of relative errors of 80 randomly sampled points used for compact model verification. (a) error in the depth approximation and (b) error in the WAHD approximation.

V. CONCLUSION

We present a physics-informed compact model for cylindrical hole etching in a SF_6/O_2 plasma. The model is integrated in a fully-fledged process simulator and is derived from a combination of experimental measurements and physical simulations. The compact model is able to reproduce the physical geometries within a reasonable error for the final depth and WAHD profiles. The average and maximum errors in the geometric feature of the cylindrical holes were found to be 1.0% and 6.2% for the etch depth, respectively, and 2.0% and 6.2% for the WAHD, respectively.

The model stores the radial features of the cylinder along its depth, meaning it is able to reproduce the most important features in the etched profile, including the sidewall tapering, bowing, and undercutting (underetching). With a speedup of more than three orders of magnitude (about 2000×), when compared to physical simulations, and reasonable accuracy, the model appears to be well suited for implementation in a DTCO flow.

ACKNOWLEDGEMENT

Financial support by the Federal Ministry of Labour and Economy, the National Foundation for Research, Technology and Development and the Christian Doppler Research Association is gratefully acknowledged.

REFERENCES

[1] G. Rzepa *et al.*, "Reliability and variability-Aware DTCO flow: Demonstration of projections to N3 FinFET and nanosheet technologies," in *Proc. IEEE IRPS*, 2021, pp. 1–7. DOI: 10.1109/irps46558.2021.9405172

[2] V. Kumbar and V. Raut, "Design and technology co-optimization for investigating power, performance, area and cost trade-offs in FinFET technologies," in *Lecture Notes in Electrical Engineering*. Springer Nature Singapore, 2022, vol. 828, pp. 623–628. DOI: 10.1007/978-981-16-7985-8_64

[3] A. Asenov *et al.*, "TCAD based design-technology co-optimisations in advanced technology nodes," in *Proc. IEEE International Symposium on VLSI-DAT*, Apr. 2017, pp. 1–2. DOI: 10.1109/vlsi-dat.2017.7939691

[4] J. Bobinac *et al.*, "Effect of mask geometry variation on plasma etching profiles," *Micromachines*, vol. 14, no. 3, pp. 665(1–16), Mar. 2023. DOI: 10.3390/mi14030665

[5] F. Roger *et al.*, "Global statistical methodology for the analysis of equipment parameter effects on TSV formation," in *Proc. IEEE VARI*, Sep. 2015, pp. 39–44. DOI: 10.1109/vari.2015.7456561

[6] L. Filipovic *et al.*, "DTCO flow for air spacer generation and its impact on power and performance at N7," *Solid-State Electronics*, vol. 199, pp. 108 527(1–5), Jan. 2023. DOI: 10.1016/j.sse.2022.108527

[7] L. Filipovic and X. Klemenschits, "Fast model for deposition in trenches using geometric advection," in *Proc. SISPAD*, Sep. 2021, pp. 224–228. DOI: 10.1109/sispad54002.2021.9592595

[8] R. J. Belen *et al.*, "Feature-scale model of Si etching in SF_6/O_2 plasma and comparison with experiments," *Journal of Vacuum Science & Technology A: Vacuum, Surfaces, and Films*, vol. 23, no. 5, pp. 1430–1439, Sep. 2005. DOI: 10.1116/1.2013317